

microdomain is surely lower than the total concentration, because DBP is distributed selectively in the PS phase. We define the effective concentration of PS in the PS phase  $C_{\text{eff}}$  by

$$C_{\text{eff}} = \frac{C_{\text{SEBS}}w_{\text{PS}} + C_{\text{PS}}}{1 - C_{\text{SEBS}}w_{\text{EB}}} \quad (3)$$

by assuming that DBP is exclusively present in the PS phase. Here  $w_{\text{PS}}$  and  $w_{\text{EB}}$  are weight fractions of PS and PEB blocks of SEBS, respectively. Equation 3 gives  $C_{\text{eff}} = 13 \text{ wt } \%$  for  $C = 30 \text{ wt } \%$ .  $D_{\text{tr}}$  of HPS in DBP solutions of HPS at  $C = 13 \text{ wt } \%$  ( $D_{\text{tr,e}}$ ) was measured under the condition that the  $M_w$  of diffusing HPS is about six times smaller than the  $M_w$  of matrix HPS and is plotted in Figure 2. The molecular weight between entanglements  $M_e$  was estimated as about 120 000 at  $C = 13 \text{ wt } \%$ .<sup>16</sup>

For diffusion in the entanglement network, we reported that in the region with  $M \leq 0.1M_e$ , the topological interaction was very small and Rouse-like behavior  $D_{\text{tr}} \propto M^{-1}$  could be observed.<sup>2</sup> Such a molecular weight dependence is also observed in the case of HPS diffusion in the SEBS solution. Moreover, it should be noticed that in the low molecular weight region, values of  $D_{\text{tr}}$  and  $D_{\text{tr,e}}$  agree very well with each other. This shows that if the molecular weight of PS is small, the effect of the SEBS matrix on the diffusing chain is very similar to that of entanglement network.

In the higher molecular region  $M_w \geq 102\,000$ , two  $D_{\text{tr}}$  values ( $D_1$  and  $D_2$ ), different by about 1 order of magnitude, indicate that two diffusion processes are present. In order to characterize these processes, more detailed FRS as well as SAXS measurements on SEBS systems with different molecular weight and concentration are in progress.

**Acknowledgment.** We are very grateful to Professor T. Hashimoto of Kyoto University for his helpful discussion. This work was partly supported by a Grant-in-Aid from the Ministry of Education, Science and Culture, Japan (Grants 59470090 and 63790323). T.I. thanks to Japan Society for the Promotion of Science for support in the form of a Fellowships for Japanese Junior Scientists.

**Registry No.** HPS, 9003-53-6; DBP, 84-74-2.

## References and Notes

- Numasawa, N.; Kuwamoto, K.; Nose, T. *Macromolecules* **1986**, *19*, 2593.
- Nemoto, N.; Okada, S.; Inoue, T.; Kurata, M. *Macromolecules* **1988**, *21*, 1509.
- Folkes, M. J.; Keller, A. In *The Physics of Glassy Polymers*; Haward, R. N., Ed.; Applied Science Publishers: London, 1973.
- Gallot, B. *Adv. Polym. Sci.* **1978**, *29*, 87.
- Here, ethylene/butylene block means an ethylene/1-butene random copolymer with 43% ethylene.
- Léger, L.; Hervet, H.; Rondelez, F. *Macromolecules* **1981**, *14*, 1732.
- Inoue, T.; Nemoto, N.; Kojima, T.; Tsunashima, Y.; Kurata, M. *Nihon Reoroji Gakkaishi* **1988**, *16*, 72 (in Japanese).
- Inoue, T.; Nemoto, N.; Kojima, T.; Tsunashima, Y.; Kurata, M. *Polym. J.* **1988**, *20*, 869.
- SEBS was labeled by using exactly the same procedure mentioned in ref 8.
- $D_e$  data from ref 7. These data are measured at  $T = 25^\circ\text{C}$ . In the discussion, the effect of the different temperature is assumed to be small.
- Hashimoto, T.; Shibayama, M.; Kawai, H.; Watanabe, H.; Kotaka, T. *Macromolecules* **1983**, *16*, 361.
- Results of more detailed analysis of lattice structure at various concentrations obtained from SAXS profiles will be described in a forthcoming paper.
- Tran-Cong, Q.; Chang, T.; Han, C. C.; Nishijima, Y. *Polymer* **1986**, *27*, 1705.
- Rhee, W. K.; Gabriel, D. A.; Johnson, C. S., Jr. *J. Phys. Chem.* **1984**, *88*, 4010.
- Zhang, J.; Wang, C. H.; Ehlich, D. *Macromolecules* **1986**, *19*, 1390.
- Calculated by using the empirical relation reported: Osaki, K.; Nishizawa, K.; Kurata, M. *Macromolecules* **1982**, *15*, 1068.

**Tadashi Inoue, Masahiro Kishine, Norio Nemoto,\* and Michio Kurata**

*Institute for Chemical Research  
Kyoto University, Uji, Kyoto-fu, 611, Japan*

*Received August 29, 1988;*

*Revised Manuscript Received November 3, 1988*

## Direct Measurement of Radical Termination in an Acrylic Copolymer by ESR and Application to Kinetic Studies

Semicontinuous emulsion polymerization is an important commercial process for the preparation of polymers by free-radical polymerization. Elucidation of the kinetics of semicontinuous emulsion polymerization is important for both fundamental understanding and practical application. ESR has previously been shown to be extremely valuable for determining the concentration of propagating free radicals and the propagation rate constant  $k_p$  for both semicontinuous emulsion polymerization<sup>1</sup> and batch emulsion polymerization.<sup>2</sup> Another parameter which is very important for understanding the polymerization kinetics is the termination rate constant  $k_t$  for the propagating free radicals. The termination rate constant directly influences the concentration of the propagating radicals in the polymer particles as expressed by

$$d[\text{R}^*]/dt = \text{entry rate} - k_t[\text{R}^*]^2 - \text{exit rate} \quad (1)$$

where  $[\text{R}^*]$  is the concentration of propagating free radicals in the polymer particles, entry rate is the rate of entry of free radicals generated in the aqueous phase into the polymer particles, and exit rate is the rate at which free radicals are desorbed from the polymer particles. If it is assumed that monomer diffusion is not rate limiting and that the bulk of the polymerization occurs in the polymer particles, then the propagating radical concentration governs the rate of polymerization according to<sup>1</sup>

$$\text{rate of polymerization} = k_p[\text{R}^*][\text{M}] \quad (2)$$

where  $[\text{M}]$  is the concentration of monomer in the polymer particles.

Despite its importance, the termination process is not well understood, and the reported rate constants are often derived from indirect measurements, which could possibly introduce significant error. The situation is especially difficult when the polymerization is in a state of high conversion such as in semicontinuous emulsion polymerization.

We have previously described<sup>1</sup> the use of ESR to directly measure the concentration of propagating free radicals in a semicontinuous emulsion polymerization of 8 BA/91 MMA/1 MAA. The polymerization was carried out by using a redox initiator system at temperatures between 50 and 65  $^\circ\text{C}$ . Samples were extracted from the reactor, and the propagating free radicals were stabilized by rapid freezing of the latices at  $-80^\circ\text{C}$ . Radical concentrations measured for particle sizes of  $\sim 50$  and  $\sim 500 \text{ nm}$  showed that the average number of radicals per particle varies greatly with particle size in this system. By use of the concentrations of the propagating free radicals measured by ESR, the propagation rate constants were calculated

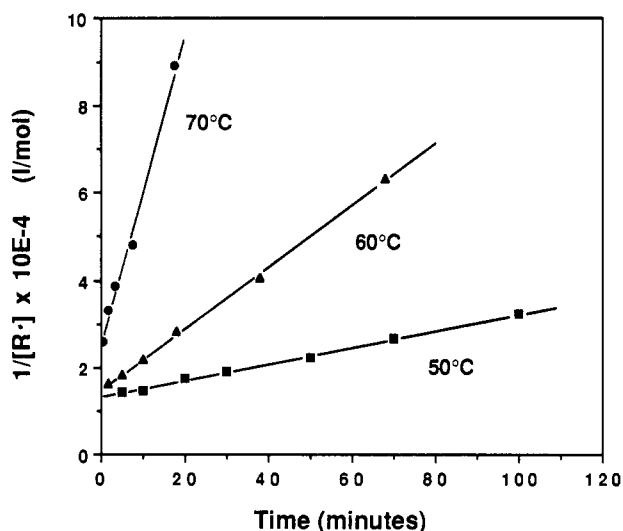


**Figure 1.** Inverse radical concentration versus time for a 500-nm latex of the acrylate copolymer treated at 50, 60, and 70 °C.

from eq 2. Different  $k_p$  values calculated for the small and large particle latices were rationalized by postulating that there is an inhomogeneity of monomer and radical concentrations in the large particle size system.

The termination rate of free radicals can be directly determined by ESR if radical generation can be stopped abruptly, and the disappearance of the radical signal is monitored. In a homogeneous polymerization system, radicals can be generated in the ESR cavity, and the disappearance rate is measured after ceasing radical generation. In our semicontinuous emulsion polymerization process, propagating radicals are generated from the redox initiator which is added into the reactor simultaneously with the monomer emulsion; the redox initiator couple then reacts at close to diffusion-controlled rates to produce radicals. The radicals generated in the aqueous phase then enter the polymer particles and initiate polymerization. When a sample is withdrawn from the reactor, addition of initiator ceases and the radical generation process stops. Our approach to measure the termination rate constant of the propagating free radicals is to use ESR to follow the disappearance of the radical signal by heating the frozen samples described above.

In studying the disappearance rate of the propagating free radicals in our acrylate copolymer, we first thawed the samples to ambient temperature; the radicals are relatively stable in the glassy polymer matrix after thawing. We typically observed some increase in the size of the radical signal for about an hour after thawing, probably due to reaction of initiator remaining at the time of sampling. All samples were maintained at ambient temperature for about an hour prior to heating and measurement of radical disappearance. Then samples were placed in a water bath at 50, 60, or 70 °C for varying periods of time. After heating, the samples were quickly refrozen, and the ESR spectra were recorded at -80 °C as described previously.<sup>1</sup> This procedure was repeated until the radical signal became weak. All thawing, heating, and freezing procedures were carried out as quickly as possible, but some error may be introduced due to the finite times required for temperature equilibration. The concentration of radicals for the untreated sample was determined by double integration of the spectrum and comparison to standards containing known concentrations of 2,2-diphenyl-1-picrylhydrazyl and 2,2,6,6-tetramethyl-1-piperidinyloxy. The concentration at various treatment times was determined by peak height comparison with the untreated sample

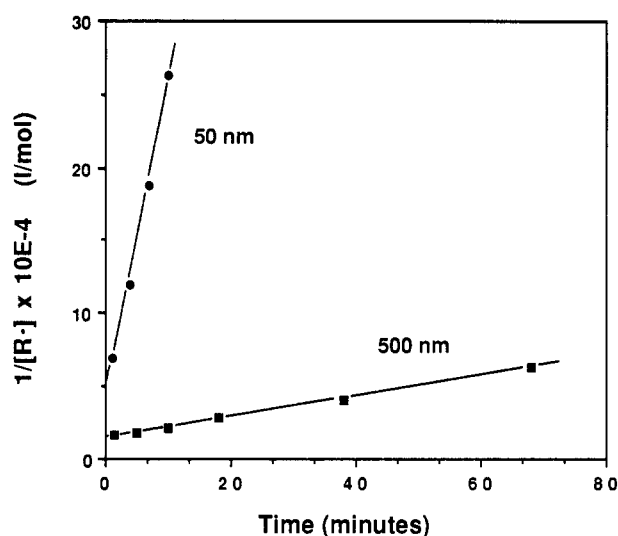


**Figure 2.** Inverse radical concentration versus time for 50-nm and 500-nm latices of the acrylate copolymer treated at 60 °C.

**Table I**  
Second-Order Rate Constants Measured for the Disappearance of MMA Propagating Radical Signals of Acrylate Copolymer<sup>a</sup>

| approx. particle size, nm | treatment temp, °C | rate const, L mol <sup>-1</sup> s <sup>-1</sup> |
|---------------------------|--------------------|---|
| 500                       | 50                 | 5   |
| 500                       | 60                 | 20  |
| 500                       | 70                 | 60  |
| 50                        | 50                 | 50  |
| 50                        | 60                 | 340   |
| 50                        | 70                 | 1600  |

<sup>a</sup> Conversion levels at the time of sampling were in the range ~95–96% for the 500-nm latices and ~96–98% for the 50-nm latices.

spectrum. We assumed that the reaction follows second-order kinetics and found that the data showed reasonable linear fits. Figure 1 shows second-order plots for 500-nm latex samples at temperatures of 50, 60, and 70 °C. The rate of disappearance of the signal clearly increases with increasing temperature. Figure 2 shows a second-order plot for both 50-nm and 500-nm particle size latices treated at 60 °C. The data show that the rate of disappearance of the propagating radical signal is significantly faster for the 50-nm particle size latex; similar data were obtained at 50 and 70 °C. Rate constants calculated from the slopes of the plots for the two particle size latices at the three temperatures are summarized in Table I. An Arrhenius plot of the results shows some scatter, but the best linear fits yield apparent activation energies of roughly 30 and 40 kcal/mol for the termination reaction of the radicals for the 500- and 50-nm particle size latices, respectively. These apparent activation energies are very high compared to those observed for typical bulk or solution polymerizations. We also observed a very high apparent activation energy (20 kcal/mol) for  $k_p$  in our previous study.<sup>1</sup>

The rate constants calculated from the ESR data for the disappearance of the propagating radical signals are orders of magnitude lower than values reported for termination in a solution polymerization or a bulk polymerization at low conversion. We attribute this difference to the very viscous nature of the highly converted polymer particles; our polymerizations are in the range of 95–98% conversion at the point when samples are removed. However, our experimental rate constants are in reasonable agreement with theoretical predictions made by Russell et al.<sup>3</sup> based

**Table II**  
Comparison of Experimental Second-Order Rate Constants with Theoretical Limits for Termination Rate Constant<sup>a</sup>

| approx. particle size, nm | second-order rate const <sup>b</sup> | theoretical termination rate const |                        |                          |                        |
|---------------------------|--------------------------------------|------------------------------------|------------------------|--------------------------|------------------------|
|                           |                                      | lower limit <sup>c</sup>           |                        | upper limit <sup>c</sup> |                        |
|                           |                                      | MMA <sup>d</sup>                   | copolymer <sup>e</sup> | MMA <sup>d</sup>         | copolymer <sup>e</sup> |
| 500                       | 5                                    | 9                                  | 14                     | 145                      | 270                    |
| 50                        | 50                                   | 3                                  | 45                     | 41                       | 780                    |

<sup>a</sup> All rate constants expressed in  $\text{L mol}^{-1} \text{s}^{-1}$  at a temperature of 50 °C. <sup>b</sup> Radical disappearance rate constants experimentally measured for the acrylate copolymer as described in the text, for both 500-nm and 50-nm latices. Average conversion levels at the time of sampling were about 95% for the 500-nm latices and about 97% for the 50-nm latices. <sup>c</sup> Upper and lower limits calculated from the equations of Russell et al.<sup>3</sup> using 95% conversion for the 500-nm latex and 97% for the 50-nm latex. <sup>d</sup> Calculated from data of Ballard et al.<sup>2</sup> for a batch emulsion polymerization of pure MMA using  $k_p = 22$  at 95% conversion and  $k_p = 12$  at 97% conversion. (We have estimated their final particle size as roughly 160 nm.) <sup>e</sup> Calculated for the acrylate copolymer (see text) using  $k_p$  values of 170 for the 50-nm latex and 35 for the 500-nm latex (values taken from Lau et al.<sup>1</sup>)

on the residual termination model. Russell et al. derived expressions for an upper limit and a lower limit for the termination rate constants in high-conversion free-radical polymerization systems. We have used their equations to calculate values for upper and lower limits for  $k_t$  for a polymerization of pure MMA at 50 °C and for our acrylate copolymer system at 50 °C to compare with the experimental data for our copolymer at that temperature; Table II summarizes the results. We have tried to make our comparisons with their theory at equivalent conversion levels, but the conversion at the time we begin the temperature treatment may be somewhat higher than the value at the time of sampling; thus, we regard our numbers and the comparison as approximate.

For both the large and small particle size systems, the experimental second-order rate constants fall near the lower limit predicted by the residual termination theory using our parameters. This trend is consistent with the behavior found by Russell et al.<sup>3</sup> at higher conversion levels. Since the experimental values are similar to those predicted by the theory, we think that the experimental second-order radical disappearance rate constants could provide a reasonable estimate for the termination rate constant during the polymerization. The interesting observation of faster termination in a 50-nm particle size latex having an average of half a radical per particle compared to that of the 500-nm particle size latex with up to 2000 radicals per particle suggests the termination step might be diffusionally controlled with chain transfer possibly involved. The postulated inhomogeneity of radical environments in the 500-nm particle size latices could also be a factor in the observed difference in termination rate. We plan further study of the termination mechanism and this difference.

Assuming our termination rate constants from the ESR study are a reasonable estimate of the termination rate of propagating radicals during the polymerization, this report to our knowledge represents the first direct experimental measurement of radical termination rate constants for an emulsion polymerization system. We can combine the termination rate constant data with our earlier results<sup>1</sup> to gain a more complete understanding of the kinetics of this system.<sup>4</sup> In future experiments, we plan to examine the propagating radicals without freezing the samples for a more direct analysis of the emulsion polymerization kinetics.

**Acknowledgment.** We thank Rohm and Haas Co. for supporting this research and permitting its publication. We are grateful to Professor D. H. Napper for helpful discussions and for sharing results prior to publication.

**Registry No.** BA, 141-32-2; MMA, 80-62-6; MAA, 79-41-4.

## References and Notes

- (1) Lau, W.; Westmoreland, D. G.; Novak, R. W. *Macromolecules* **1987**, *20*, 457.
- (2) Ballard, M. J.; Gilbert, R. G.; Napper, D. H.; Pomery, P. J.; O'Sullivan, P. W.; O'Donnell, J. H. *Macromolecules* **1986**, *19*, 1303.
- (3) Russell, G. T.; Napper, D. H.; Gilbert, R. G. *Macromolecules* **1988**, *21*, 2133.
- (4) Direct elucidation of major kinetic parameters ( $k_p$ ,  $k_t$ , initiator efficiency, and activation energy) will be discussed more fully in a separate report.

David G. Westmoreland and Willie Lau\*

Research Laboratories, Rohm and Haas Company  
Spring House, Pennsylvania 19477

Received August 30, 1988;

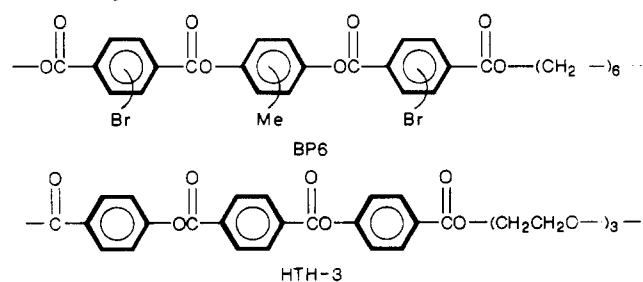
Revised Manuscript Received November 2, 1988

## Studies of Liquid Crystalline Polymer Phase Transitions Using Synchrotron X-Radiation

Little more than a decade ago liquid crystallinity in polymers was first recognized. Since that time the numbers and types of newly synthesized liquid crystalline polymers (LCPs) have increased rapidly. A number of entirely aromatic LCPs, which are thus stiff and insoluble, have recently been commercialized. In addition to the commercial polymers, many polymers containing both mesogenic units and flexible spacers have been the subject of extensive study around the world. The mesogenic units and flexible spacers either may appear in the main polymer chain or the mesogenic units may be attached by spacers to a polymer backbone in the so-called side-chain LCPs. The use of flexible spacers has also resulted in the lowering of melting points in LCPs, and more recently substituents have been added to the mesogenic groups thereby inducing solubility in common organic solvents while maintaining the LC properties.<sup>1,2</sup>

We have become interested in the physical nature of the mesophase and in studying the mesophase transitions of model LCPs. In this paper we describe recent studies of LCP mesophases and mesophase transitions studied by using real-time X-ray diffraction experiments made possible by the use of synchrotron radiation. Specifically, variations in X-ray diffracted intensities were used to follow transitions from the LCP mesophase to the isotropic melt. We were interested in studying not only the rate of transition but also the biphasic behavior of selected liquid crystalline polymers.

The mesogenic structures of the LCPs investigated in this study are shown below:



The BP6 polymer with a spacer composed of 6 methylene units is unusual in that it has an irregular mesogenic